

Pairwise Dynamic Time Warping for Event Data

Ana Arribas-Gil

Departamento de Estadística

Universidad Carlos III de Madrid, Getafe, Spain.

E-mail: aarribas@est-econ.uc3m.es

Hans-Georg Müller

Department of Statistics, University of California, Davis

Davis, CA 95616 USA

Abstract

We introduce a new version of dynamic time warping for samples of observed event times that are modeled as time-warped intensity processes. Our approach is developed within a framework where for each experimental unit or subject in a sample, one observes a random number of event times or random locations. As in our setting the number of observed events differs from subject to subject, usual landmark alignment methods that require the number of events to be the same across subjects are not feasible. We address this challenge by applying dynamic time warping, initially by aligning the event times for pairs of subjects, regardless of whether the numbers of observed events within the considered pair of subjects match. The information about pairwise alignments is then combined to extract an overall alignment of the events for each subject across the entire sample. This overall alignment provides a useful description of event data and can be used as a pre-processing step for subsequent analysis. The method is illustrated with a historical fertility study and with on-line auction data.

Keywords: Alignment, Birth data, French-Canadian fertility, Functional data analysis, On-line auctions, Point process, Registration

1 Introduction

Time warping is commonly used in functional data analysis to address the presence of random variation in time in addition to amplitude variation. A major difficulty is the non-identifiability of these two components (Liu and Müller 2004). This non-identifiability requires that one makes strong assumptions on the nature of the warping mechanism in order to be able to distinguish it from the variation in the random amplitudes. While various solutions have emerged over the years, a gold standard for functional time warping is the landmark method (Kneip and Gasser 1992; Gasser and Kneip 1995). In this method, one typically extracts for each random curve X_i in a sample of i.i.d. trajectories X_1, \dots, X_n a series of landmarks, which correspond to the times or locations where certain features occur, such as the location of a zero or the location of a peak.

One then uses these locations to represent the sample or for subsequent continuous time warping of the random functions, by moving the landmark locations to their cross-sample average locations. Then one can smoothly map the time intervals in between these locations, for example by applying monotone spline transformations. Usually, the landmarks are obtained by presmoothing the often noisily observed functions X_i , obtaining estimates \hat{X}_i and then extracting features such as peak locations by substituting the unknown peak location $\theta_i = \operatorname{argmax}_x X_i(x)$ by the estimated peak location $\hat{\theta}_i = \operatorname{argmax}_x \hat{X}_i(x)$, where a peak is just one of many possible features defining a landmark (Gasser et al. 1984b).

A persistent difficulty with the landmark method has been that in real data applications, landmarks such as peaks can be hard to identify for specific sample curves, due to either noise in the measurements or to the presence of non-standard trajectories, which do not exhibit some of the landmarks or have more landmarks. In growth curves, for example, one might encounter more than one mid-growth spurt

and it is then hard to decide how to position extra peaks within the sequence of landmarks. The landmark method however requires that the number of identified landmarks matches across all curves and also that the landmarks are in a sequence that is equally interpretable across all subjects in terms of features (location of peaks and of zeros and size of peaks for functions and derivatives). In addition, although seemingly straightforward, the computational task of landmark extraction is actually quite burdensome and usually cannot be fully automated, so that identifying and verifying a large number of landmarks even for modest samples of curves can be a major effort that includes some subjective elements (Gasser et al. 1984a).

For these reasons, non-landmark based methods for function warping have met with increasing interest in recent years in the functional data analysis literature (Silverman 1995; Wang and Gasser 1997; Aach and Church 2001; Rønn 2001; Gervini and Gasser 2004; Kneip and Ramsay 2008; Telesca and Inoue 2008). As already mentioned, such methods depend explicitly or implicitly on strong assumptions to circumvent the non-identifiability problem. In this paper, we take a different approach. We assume from the beginning that the number of landmarks that can be identified in sample trajectories is random, but that nevertheless their order matters, so that the lower ranked landmarks should be placed closer together in time than the higher ranked landmarks, irrespective of the number of landmarks that are available for each subject.

More generally, the times at which landmarks occur are viewed as random event times that are observed for each subject. These event times carry information about their order and relative location to each other, but otherwise are not distinguishable. Typical examples for such event data that we use to illustrate our methods are age at child birth per woman in a large French-Canadian historical cohort, where women typically have a large number of offspring, and the timings of bids submitted at online e-bay auctions, recorded for each auction in a sample of auctions. Such data can be viewed as realizations of random intensities of underlying point processes. Related methods for time synchronization for densities have been studied in Zhang and Müller (2011); for general functional methodology for intensities we refer to Bouzas et al. (2006); Wu and Zhang (2012).

To model such data, denote the n_i observed event times for the i -th subject

by t_{i1}, \dots, t_{in_i} , and assume that all event times are observed within the interval $\mathcal{T} = [0, T]$. We consider standardized cumulative incidence functions

$$Y_i(t) = \frac{1}{n_i} \sum_{j=1}^{n_i} 1_{\{t_{ij} \leq t\}}, \quad t \in \mathcal{T}, \quad i = 1, \dots, n,$$

and assume these are generated by an underlying monotone increasing fixed function μ and warping functions h_i , which are i.i.d. realizations of a random variable H taking values on $\mathcal{W}(\mathcal{T}) = \{f \in \mathcal{C}(\mathcal{T}) \mid f \text{ strictly increasing, } f(0) = 0, f(T) = T\}$, such that

$$Y_i(t_{ij}) = \mu(h_i^{-1}(t_{ij})), \quad t_{ij} \in \mathcal{T}, \quad i = 1, \dots, n, \quad j = 1, \dots, n_i. \quad (1)$$

Here, $\mu(t)$ is a cumulative distribution function and the constraints on H ensure that $\mu(h_i^{-1}(t))$ also are (random) cumulative distribution functions. In this framework, registration procedures are defined by estimates of the registration functions h_i . The determination of the time warping functions h_i is of intrinsic interest and also allows to determine unwarped versions $X_i(t) = Y_i(h_i(t))$, $t \in \mathcal{T}$ of the Y_i . For identifiability purposes, it is expedient to assume that $\mathbb{E}[H(t)] = I_{\mathcal{T}}(t)$, where $I_{\mathcal{T}}$ is the identity function on the domain \mathcal{T} .

2 Methodology

2.1 Pairwise registration

For pairwise registration, we adopt the approach proposed by Rong and Müller (2008). The idea is to obtain global alignment for a sample of random functions, from information about pairwise alignments. Using this device, the task of global registration is reduced to the often more manageable task of constructing pairwise or “relative” alignments between pairs of random trajectories.

The initial goal is thus to obtain pairwise synchronizations for all or many pairs of curves Y_i and Y_j , as defined in (1). For this purpose, Rong and Müller (2008)

define pairwise synchronization functions

$$g_{ji}(t) = h_j(h_i^{-1}(t)), \quad (2)$$

which provide a transformation of the time scale of the curve Y_j towards that of Y_i , and show that $\mathbb{E}[h_j(h_i^{-1}(t))|h_i^{-1}(t)] = h_i^{-1}(t)$. This motivates the estimators

$$\hat{h}_i^{-1}(t) = \frac{1}{n-1} \sum_{j \neq i} \hat{g}_{ji}(t). \quad (3)$$

The alignment problem is then reduced to the problem of defining appropriate estimators $\hat{g}_{ji}(t)$, that can take into account the particular nature of the data, in our case event data. While Rong and Müller (2008) proposed minimization of a penalized L^2 -distance to obtain appropriate estimates of $g_{ji}(t)$, in the situation we study here, dynamic time warping (DTW) provides a promising alternative.

2.2 Dynamic time warping

Dynamic time warping (DTW) is a series of alignment algorithms originally developed in the 1970s in the context of speech recognition (see Kruskal and Liberman (1983) for an overview). These are dynamic programming algorithms that, given a certain metric, consist on aligning two sequences of outcomes by minimizing the total distance between them, computed as the sum of distances between each pair of points along the aligned positions in a suitable metric. Dynamic time warping is similar to the algorithms used for the alignment of biological sequences, such as the Needleman-Wunsch algorithm (Needleman and Wunsch 1970) for global alignment.

In this context, given two sequences $\mathbf{a} = (a_1, \dots, a_\ell)$ and $\mathbf{b} = (b_1, \dots, b_m)$, with values on a certain feature space \mathcal{A} , an alignment of \mathbf{a} and \mathbf{b} is a sequence $\{\varepsilon_k\}_{k=1}^{|\varepsilon|}$ of variable length $|\varepsilon|$, taking values on $\{(0, 1), (1, 0), (1, 1)\}$ such that $\sum_{k=1}^{|\varepsilon|} \varepsilon_k = (\ell, m)$. That is, $(L_r, M_r) = \sum_{k=1}^r \varepsilon_k$, $r = 1, \dots, |\varepsilon|$, defines a path from $(0, 0)$ to (ℓ, m) in the two-dimensional integer lattice. We say that a_i is aligned to b_j if there exists a $1 \leq r \leq |\varepsilon|$ such that $\sum_{k=1}^r \varepsilon_k = (i, j)$. Thus in dynamic time warping one allows one

element in one sequence to be aligned to more than one element in the other sequence, which makes this method suitable for sequences of event times with unequal number of events in each sequence. The general approach is illustrated in Figure 1.

In our setting of event data, we observe pairs of curves $\mathbf{a} = (Y_i(t_{i1}), \dots, Y_i(t_{in_i}))$ and $\mathbf{b} = (Y_j(t_{j1}), \dots, Y_j(t_{jn_j}))$ at event times $\mathbf{t} = (t_{i1}, \dots, t_{in_i})$ and $\mathbf{s} = (t_{j1}, \dots, t_{jn_j})$, respectively. Then, to align curves Y_i and Y_j one needs to determine, first, which elements of the sequence \mathbf{a} should be mapped to which elements of the sequence \mathbf{b} , and second, the time points at which these aligned values should be placed. For the first determination, a discrete DTW approach, which is described next, is used. The second determination is addressed in Section 2.3.

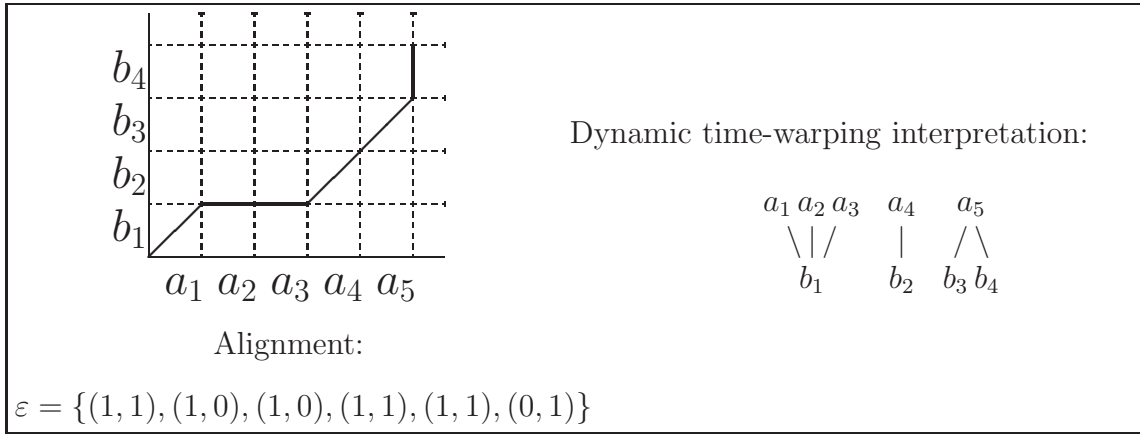


Figure 1: Graphical representation of a dynamical time warping alignment between two sequences $\mathbf{a} = (a_1, \dots, a_\ell)$ and $\mathbf{b} = (b_1, \dots, b_m)$. Lines represent correspondence between elements of the two sequences.

From now on and in the following, we use the notation $\mathbf{a} = (a_1, \dots, a_\ell)$ and $\mathbf{b} = (b_1, \dots, b_m)$ to refer to the observed values, without any temporal reference, of any pair of curves. We now describe the DTW algorithm that allows us to find an optimal mapping between these two sequences.

Let $d : \mathcal{A} \times \mathcal{A} \rightarrow \mathbb{R}$ be a suitable distance function defined on the feature space.

Then, for any alignment ε , its alignment distance is given by

$$D_\varepsilon(\mathbf{a}, \mathbf{b}) = \sum_{k=1}^{|\varepsilon|} w(k) \cdot d(a_{L_k}, b_{M_k}), \quad (4)$$

where $w(\cdot)$ represents time weights that account for the length of the alignment. Different definitions of these weights are possible, even $w(\cdot) = 1$ (see Wang and Gasser (1997) for the study of weight functions in the continuous time DTW problem). In this work we consider the definition given by Kruskal and Liberman (1983), $w(k) = (t_{L_k} - t_{L_{k-1}} + s_{M_k} - s_{M_{k-1}})/2$, which is quite standard in the DTW literature.

Then, the optimal alignment is

$$\varepsilon^{ab} = \arg \min_{\varepsilon \in \mathcal{E}_{\ell, m}} D_\varepsilon(\mathbf{a}, \mathbf{b}), \quad (5)$$

where $\mathcal{E}_{\ell, m}$ is the set of all possible alignments of sequences with lengths ℓ and m . The dynamic time-warping algorithm used to retrieve ε_{ab} is as follows:

1. Initialize:

$$\begin{aligned} D_{(1,1)} &= 0, & I_{(1,1)} &= (1, 1), \\ D_{(i,1)} &= D_{(i-1,1)} + d(a_i, b_1) \cdot (t_i - t_{i-1})/2, & I_{(i,1)} &= (1, 0), \quad i = 2, \dots, \ell, \\ D_{(1,j)} &= D_{(1,j-1)} + d(a_1, b_j) \cdot (s_j - s_{j-1})/2, & I_{(1,j)} &= (0, 1), \quad j = 2, \dots, m. \end{aligned}$$

2. Iterate for $i = 2, \dots, \ell, j = 2, \dots, m$:

$$D_{(i,j)} = \min \begin{cases} D_{(i-1,j-1)} + d(a_i, b_j) \cdot \frac{(t_i - t_{i-1} + s_j - s_{j-1})}{2} \\ D_{(i-1,j)} + d(a_i, b_j) \cdot \frac{(t_i - t_{i-1})}{2} \cdot \mathbb{1}\{I_{(i-1,j)} \neq (0, 1)\} + M \mathbb{1}\{I_{(i-1,j)} = (0, 1)\} \\ D_{(i,j-1)} + d(a_i, b_j) \cdot \frac{(s_j - s_{j-1})}{2} \cdot \mathbb{1}\{I_{(i,j-1)} \neq (1, 0)\} + M \mathbb{1}\{I_{(i,j-1)} = (1, 0)\} \end{cases}$$

$$I_{(i,j)} = \begin{cases} (1, 1) & \text{if } D_{(i,j)} = D_{(i-1,j-1)} + d(a_i, b_j) \cdot \frac{(t_i - t_{i-1} + s_j - s_{j-1})}{2} \\ (1, 0) & \text{if } D_{(i,j)} = D_{(i-1,j)} + d(a_i, b_j) \cdot \frac{(t_i - t_{i-1})}{2} \\ (0, 1) & \text{if } D_{(i,j)} = D_{(i,j-1)} + d(a_i, b_j) \cdot \frac{(s_j - s_{j-1})}{2} \end{cases}$$

3. $d_{\varepsilon^{ab}}(\mathbf{a}, \mathbf{b}) = D_{(\ell, m)}$.

4. Trace back:

$\varepsilon_{|\varepsilon^{ab}|}^{ab} = I_{(\ell, m)}$, $i = \ell - I_{(\ell, m)}(1)$, $j = m - I_{(\ell, m)}(2)$, $k = |\varepsilon^{ab}|$ and while $i \geq 1$ and $j \geq 1$ do:

$$\begin{aligned} \varepsilon_k^{ab} &= I_{(i, j)}, \quad k = k - 1, \\ i &= i - I_{(i, j)}(1), \quad j = j - I_{(i, j)}(2). \end{aligned} \tag{6}$$

Note that in step 1, the initialization $D_{(1,1)} = 0$, $I_{(1,1)} = (1, 1)$, forces the two first values of the two sequences to be aligned together. In step 2, we prevent having a vertical movement followed by an horizontal one, or vice versa, by choosing a sufficiently large constant M . This means that if for instance a_i, \dots, a_{i+k} , $k > 0$, are all mapped to b_j , then b_{j+1} can not be mapped again to a_{i+k} . As for the computational cost, it is $\mathcal{O}(\ell \cdot m)$, which is low, since ℓ and m , the number of events per curve, are usually quite small.

Once we obtain the optimal alignment, ε^{ab} , of sequences \mathbf{a} and \mathbf{b} , what we get is a correspondence between values a_1, \dots, a_ℓ and b_1, \dots, b_m , without any timing reference. That is, at this stage we do not tackle the problem of designating the time points at which two (or more) aligned values should be placed. This is a major difference between our approach and previous work using DTW related algorithms in the context of time warping, as for example Wang and Gasser (1997, 1999). Indeed, these works deal with continuous features and time synchronization problems in which finding similarities between points in different curves and assigning temporal references cannot be tackled separately. In Bigot (2006), a dynamic programming algorithm similar to (6) is used to find a correspondence between two previously identified sets of landmarks from two curves. Then, a penalized least squares minimization problem is solved to estimate the warping functions that register the two curves through the alignment of their landmarks.

Our approach is quite different since we focus on global alignment of the whole set of curves for which pairwise alignment maps constitute just a preliminary stage. That is, we use DTW to determine the pairwise correspondence of events, and this

information about pairwise correspondences is then combined (see Section 2.3) to obtain global alignment, i.e., to register the entire sample. This is a key difference, as the main disadvantage of DTW based registration methods is that the generalization from two to a larger number of curves is not straightforward. Indeed, extensions to the alignment of a larger set of curves usually lie in defining a common set of landmarks (from individual landmark vectors or from a template curve) to which then the entire sample of curves is aligned. However, this ad hoc approach suffers from a loss of information and requires computationally intensive algorithms.

In the last decade, DTW has been used for the alignment of expression profiles from time-course microarray experiments (see Aach and Church (2001) and Clote and Straubhaar (2006)). In this context, a n -dimensional time series, containing the expression levels of a group of n genes recorded at the same time points (and which are assumed to be synchronized), is aligned to another n -dimensional time series corresponding to a different microarray experiment of the same n genes. That is, DTW is used to perform pairwise alignment of two n -dimensional sequences. This is different from using DTW to align n different trajectories. Indeed, although multiple dynamic time warping is theoretically possible and algorithmically equivalent to the pairwise case, it is computationally unfeasible even for a relatively small number of sequences, since the computing time is proportional to ℓ^n , where n represents here the total number of sequences and ℓ their length, assuming they all have similar lengths.

2.3 Pairwise dynamic time warping

The proposed strategy is to combine DTW, to obtain pairwise alignment maps in a first step, with pairwise registration. The goal is to extract information about global alignment from the pairwise correspondences.

Then, given a sample of n curves, we aim at estimating $\hat{g}_{ij}(t)$ and $\hat{g}_{ji}(t)$ for any $i, j = 1, \dots, n$. The observations in model (1) are (t_{ik}, y_{ik}) , $k = 1, \dots, n_i$, $i = 1, \dots, n$, where t_{ik} is the time at which the k -th event is observed for individual i and y_{ik} is the observed value of Y_i at time t_{ik} .

However, in what follows we will focus on any given pair of curves y_i and y_j , and for the sake of simplicity will denote the corresponding observations as (t_k, y_{ik}) , $k = 1, \dots, n_i$ and (s_k, y_{jk}) , $k = 1, \dots, n_j$. Applying algorithm (6) we obtain an optimal mapping, ε^{ij} , of the values y_i and y_j . But one thing is to decide which values on both sequences can be aligned together, and another thing is to decide the time points corresponding to the aligned records. However, recall that in our case the alignment of pairs of curves is just a preliminary step to arrive at a global alignment of the whole sample of curves and is not an objective by itself. From estimated pairwise alignments $\hat{g}_{ji}(t)$ and $\hat{g}_{ij}(t)$, we also obtain $\hat{g}_{ji}(t_k) = s_h$ and $\hat{g}_{ij}(s_h) = t_k$. However, if more than one value in one curve is mapped to the same single value in the other curve some additional considerations are needed.

We now describe the detailed procedure to obtain $\hat{g}_{ij}(t)$ and $\hat{g}_{ji}(t)$ from observed sequences (t_k, y_{ik}) , $k = 1, \dots, n_i$, and (s_k, y_{jk}) , $k = 1, \dots, n_j$:

- Find ε^{ij} , the optimal alignment between the two sequences applying algorithm (6) with d being the Euclidean distance in \mathbb{R} . Denote $p = |\varepsilon^{ij}|$.

- $(L_{1:p}, M_{1:p}) = \left\{ \sum_{k=1}^r \varepsilon_k^{ij} \right\}_{r=1, \dots, p}$.

- $\alpha_1 = M_1$ and $\alpha_{2:n_i} = \{M_s, s = 2, \dots, \ell, \text{ s.t. } L_s \neq L_{s-1}\}$
 $\beta_1 = L_1$ and $\beta_{2:n_j} = \{L_s, s = 2, \dots, \ell, \text{ s.t. } M_s \neq M_{s-1}\}$.

- For $k = 1 \dots, n_i$:

$$\begin{aligned}
 t_k^* &= s_{\alpha_k} && \text{if } \alpha_{k-1} \neq \alpha_k \neq \alpha_{k+1} \text{ (only one of them if } k = 1 \text{ or } n_i) \\
 t_{k+h}^* &= s_{\alpha_k} - l + \frac{2l}{H-1}h, && h = 0, \dots, H-1, \text{ with } l = \frac{\delta(t_{k+H-1} - t_k)}{2} \\
 &&& \text{if } \alpha_{k-1} \neq \alpha_k = \alpha_{k+1} = \dots = \alpha_{k+H-1} \neq \alpha_{k+H}
 \end{aligned} \tag{7}$$

- For $k = 1 \dots, n_j$:

$$\begin{aligned}
 s_k^* &= t_{\beta_k} && \text{if } \beta_{k-1} \neq \beta_k \neq \beta_{k+1} \text{ (only one of them if } k = 1 \text{ or } n_j) \\
 s_{k+h}^* &= t_{\beta_k} - l + \frac{2l}{H-1}h, && h = 0, \dots, H-1, \text{ with } l = \frac{\delta(s_{k+H-1} - s_k)}{2} \\
 &&& \text{if } \beta_{k-1} \neq \beta_k = \beta_{k+1} = \dots = \beta_{k+H-1} \neq \beta_{k+H}
 \end{aligned} \tag{8}$$

- Define

$$\hat{g}_{ji}(t_k) = t_k^*, \quad k = 1, \dots, n_i \quad \hat{g}_{ij}(s_k) = s_k^*, \quad k = 1, \dots, n_j. \quad (9)$$

Note that expressions (7) and (8) correspond to an interpolation step in the cases in which more than one value of y_i has been assigned to the same single value of y_j and vice versa. In those cases, we spread those values in a certain interval rather than bringing them together to the same time point. That is, if values $y_{ik}, \dots, y_{i,k+H-1}$ are all mapped to y_{j,α_k} , instead of defining $\hat{g}_{ji}(t_{k+h}) = s_{\alpha_k}$, $h = 0, \dots, H-1$, we equally distribute these points around w_{α_k} in such a way that the slope of \hat{g}_{ji} between t_k and t_{k+H-1} is equal to δ (where δ is a parameter that needs to be chosen in advance). In this way we guarantee that the estimates $\hat{g}_{ji}(t)$ and $\hat{g}_{ij}(t)$ are strictly increasing. This is illustrated in Figure 2.

Once we have discrete time estimates of $g_{ji}(t)$ and $g_{ij}(t)$, for any pair $i, j = 1, \dots, n$, $i \neq j$, following Rong and Müller (2008) we define:

$$\hat{h}_i^{-1}(t_k) = \frac{1}{n-1} \sum_{j \neq i} \hat{g}_{ji}(t_k), \quad k = 1, \dots, n_i, \quad i = 1, \dots, n. \quad (10)$$

We note here that each estimated warping function, \hat{h}_i^{-1} , is only defined over the grid of observed event times of its corresponding curve, y_i . The same applies for the estimated registered curves $\hat{x}_i = y_i \circ \hat{h}_i$. Then, any further step involving computations with either the estimated warping functions or registered curves, such as calculating the sample mean of the registered curves for instance, requires an additional interpolation step aiming to anchor curves at a common grid of time points.

As for the computational complexity of the pairwise dynamic time warping algorithm to produce an alignment of a set of n curves, this is proportional to $\binom{n}{2} \ell^2 \approx (n \cdot \ell)^2$, (ℓ standing for some average number of events). This represents a very important reduction compared to the dynamic time warping approach for multiple alignment, which has a computational cost of $\mathcal{O}(\ell^n)$, as we have already mentioned.

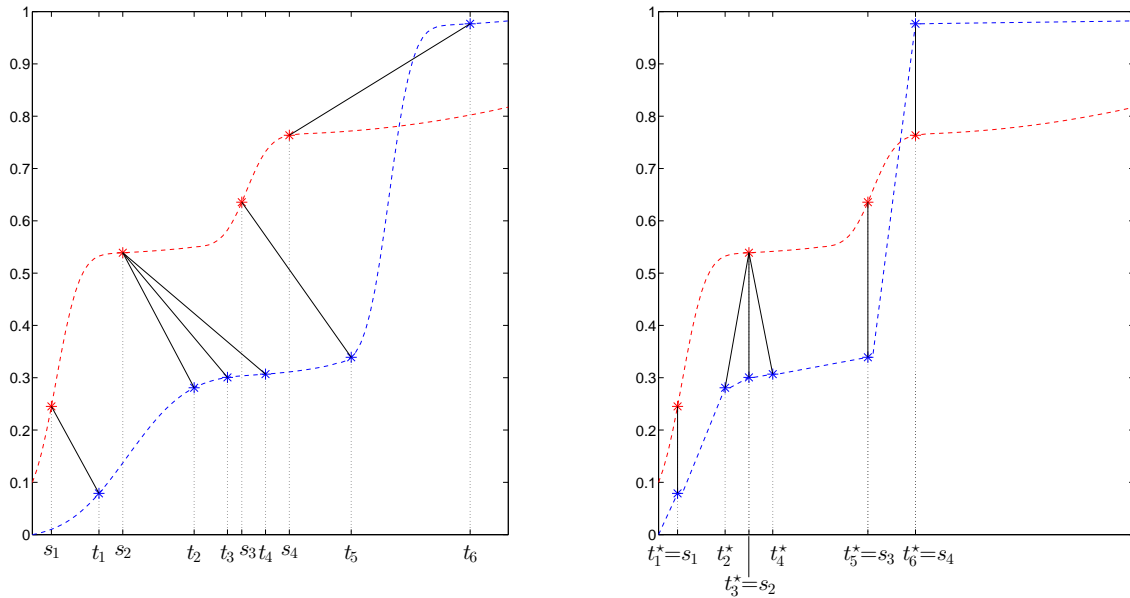


Figure 2: Left: Blue stars are points (t_k, y_{ik}) and red stars are points (s_k, y_{jk}) . Solid black lines represent the alignment obtained by DTW. Imaginary continuous trajectories are displayed in dashed lines, although these are not observed in practice. Right: Alignment of y_i towards y_j . Blue stars are now points $(t_k^* = \hat{g}_{ji}(t_k), y_{ik})$. Points (t_2, y_{i2}) , (t_3, y_{i3}) , (t_4, y_{i4}) although all mapped to (s_2, y_{j2}) , are spread in a small interval around s_2 .

3 Applications

3.1 Historical fertility data

We study fertility from a well-documented 17/18th century cohort of 1877 native born French-Canadian women who lived past age 50. This data contain the number of children and the age at the different births for each woman in the sample. We consider only those women with more than one child; the resulting data consist of 1810 individuals. For more details on this data set see Müller et al. (2002) and the references therein.

To study the relation between the total number of children and the dynamics of the giving birth process, we transform the data to obtain a curve (t_{ik}, y_{ik}) , $i =$

$1, \dots, n_i$ for each woman, where t_{ik} is the age of the i -th woman at her k -th birth, $y_{ik} = k$ and n_i is her total number of children. The time domain is $\mathcal{T} = [13.7, 50.2)$, units are years. To anchor all sample curves on this interval, we add points $(13.7, 0)$ and $(50.2, n_i)$ at the beginning and at the end of each curve. Since this introduces an artificial constant fragment at the end of each curve an important reference is the age at the last birth for each woman and not the end of the interval, we force points (t_{in_i}, y_{in_i}) , $i = 1, \dots, n$, to be mapped together. The whole sample before and after registration by the procedure described in Section 2.3 is presented in Figure 3. Note that the registered sample includes contracted time domains for some women so that the periods between births may be shorter than 9 months. This is a consequence of the forced alignment at the first and last births across all women and is also reflected in some of the mean group intensity functions (averages of the registered curves for women with the same number of offspring) displayed in Figure 4. Nevertheless, the mean intensity function for the whole sample presents a good approximation of the standard fertility process and captures a linear trend along with the mean ages at the first and last birth, which are 22.4 and 40.2 years respectively. In the case of the sample mean of the original trajectories (Figure 4), these ages are under-, respectively, over-estimated. After registration, the estimated warping functions can be used for classification purposes. We consider a distance-based approach by defining individual distances from the warping functions as follows,

$$d(i, j) = \int_{\mathcal{T}} \left(\hat{h}_i^{-1}(t) - \hat{h}_j^{-1}(t) \right)^2 dt, \quad i, j = 1 \dots, n. \quad (11)$$

Indeed, since the warping functions are strictly increasing and defined from \mathcal{T} to \mathcal{T} , the area between two of these functions is a good indicator of the difference in the degree of time distortion that they introduce in the respective individual curves. We expect that this distance will be useful at discriminating between different fertility dynamics. This distance matrix needs to be computed numerically from the discrete-valued warping function estimates.

Unlike common approaches in functional data analysis, we propose to perform clustering directly from the distance matrix without any previous step to reduce

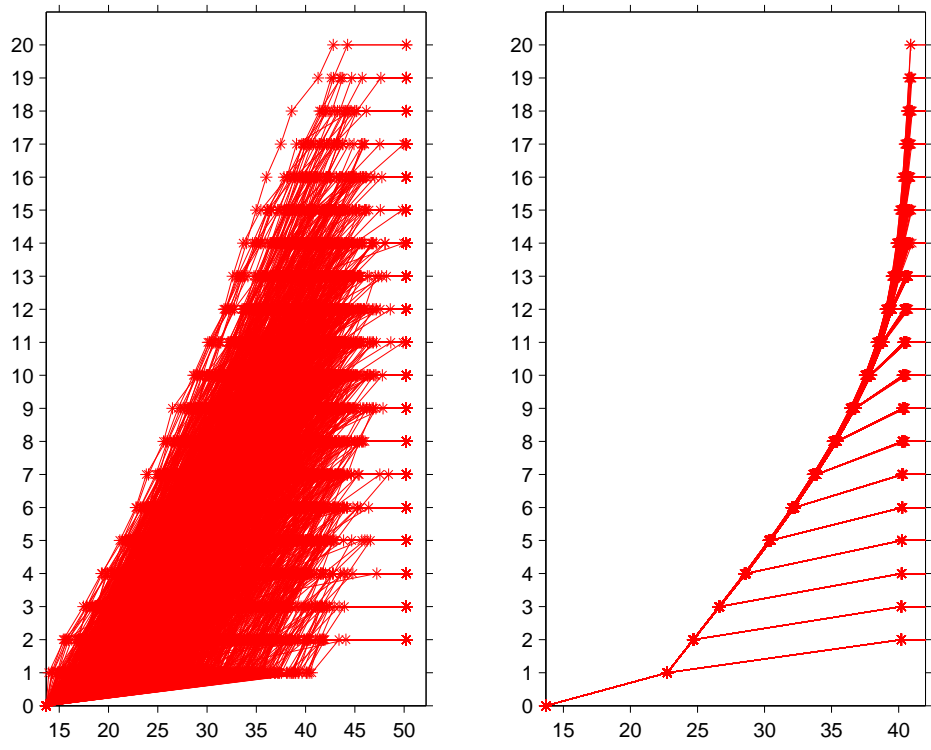


Figure 3: Left: Absolute number of children along time for 1810 women. Stars represent the observed data, solid lines are obtained by connecting births within each record. Right: Absolute number of children versus registered births times for 1810 women.

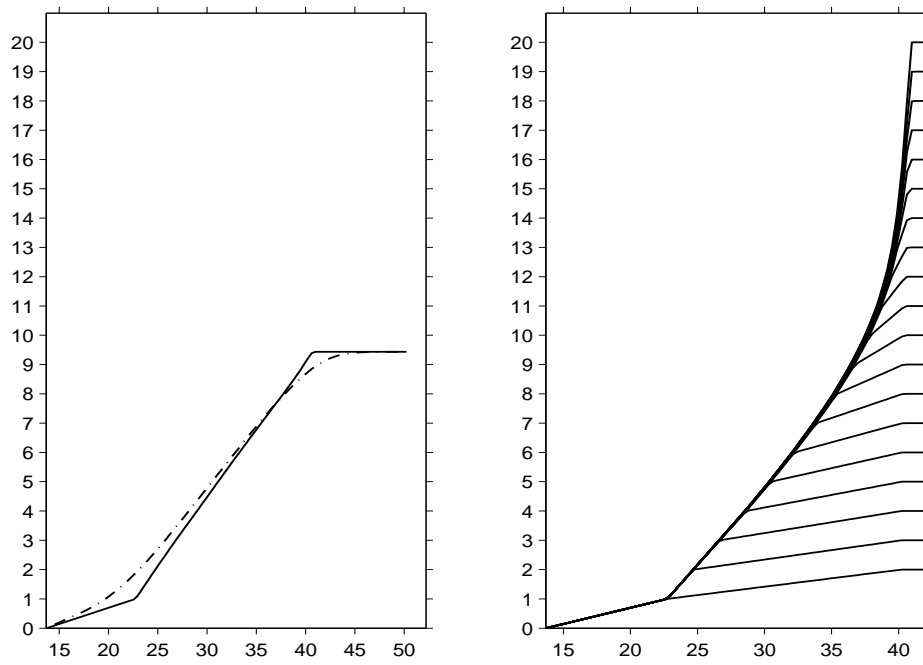


Figure 4: Left: Mean intensity function before (dashed-dotted line) and after registration (solid line). Right: Group mean intensity functions. The groups are defined by the women with the same number of children.

the dimensionality of the data. The clustering method is a modified version of the k-means algorithm in which the centroid of a group G , is calculated as its Fréchet mean, $c_G = \operatorname{argmin}_{x \in G} \sum_{y \in G} d^2(x, y)$. To choose the number of clusters we use the *silhouette* coefficient (Kaufman and Rousseeuw 1990) that for each individual provides a measure of how well classified it is. The *silhouette* of individual i is $(b_i - a_i) / \max\{a_i, b_i\}$, where a_i is the mean distance of i to the rest of individuals in the same cluster and b_i is the mean distance of i to the individuals of the closest cluster (besides the one it is assigned to). Finally, the *silhouette* coefficient of a clustering is the mean *silhouette* across individuals. Then, the choice of the number of clusters is done by maximizing the *silhouette* coefficient. For this data set, the maximum was found for $k = 2$ clusters, with a value of 0.60. According to Kaufman and Rousseeuw (1990), a value of this coefficient between 0.51 and 0.70 indicates that a reasonable structure has been found in the data.

The results for $k = 2$ clusters are displayed in Figure 5. The two clusters can be defined as women with late birth trajectories, and women with regular birth trajectories. A regular birth trajectory is almost linear, the first birth occurring in average at 20.8 years and the last birth at 39.7 years. In contrast, a late birth trajectory is piecewise linear with two differentiated pieces, the first one with lower slope than the second one. In fact the slope of the second fragment is similar to that of a regular trajectory. The average ages at the first and last birth for women in this category are 29.4 and 41.8 years. Then, we can say that the main difference between the women in the two clusters is the age at which the first child is born, since after the first birth, the fertility process looks similar in both cases. If we now look at the distribution of the number of children in these two clusters we observe an expected consequence, namely, that the total number of children is generally lower for those women that had their first child at an older age.

3.2 Online auction data

Modelling of price paths in on-line auction data has received a lot of attention in recent years (Shmueli and Jank 2005; Jank and Shmueli 2006; Shmueli et al. 2007;

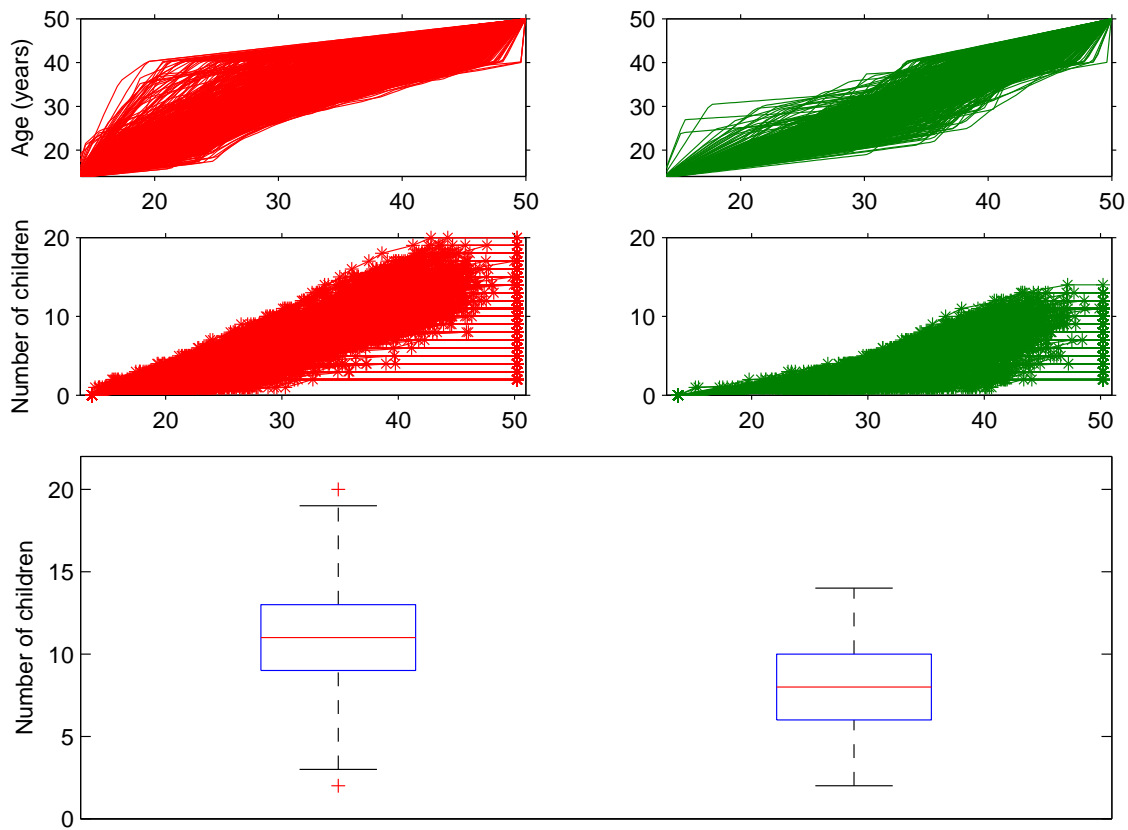


Figure 5: Warping function estimates (\hat{h}_i^{-1}), fertility curves and box plots of the number of children for the two clusters.

Liu and Müller 2008). One of the reasons is the availability of huge amounts of data made public by the on-line auction and shopping website eBay.com, which has become a global market place in which millions of people worldwide buy and sell products. The price evolution during an auction can be thought as a continuous process which is observed discretely and sparsely only at the instants in which bids are placed. In fact, bids tend to concentrate at the beginning and at the end of the auction, corresponding to two typically observed phenomena, “early bidding” and “bid sniping” (a situation in which “snipers” place their bids at the very last moment). Here, we analyze a set of 158 eBay auctions for Palm M515 Personal Digital Assistants (PDA), of a fixed duration of seven days, that took place between March and May, 2003. This data set is publicly available at <http://www.rhsmith.umd.edu/digits/statistics/data.aspx> and has been previously studied by Shmueli and Jank (2005) and Liu and Müller (2008), among others. As in Liu and Müller (2008) we restrict our analysis to 156 auctions after removing two irregular recordings.

Our interest here is not focused on the price process, but rather on the intensity functions that quantify the bid arrivals along the time axis, where each bid arrival generates an event time. This approach may be useful to understand different bidding behaviors and for characterizing the bid arrivals process. A characteristic of these data is that bidding trajectories for different auctions are quite dissimilar. While most of them reflect very low bidding activity at the beginning of the auction and intense bidding when the auction is near its end, in other auctions one observes different patterns. It seems reasonable to view these trajectories as accelerated and decelerated versions of an underlying bidding intensity function and therefore the proposed time warping model seems suitable for this analysis.

The time domain for observations is $\mathcal{T} = [0, 168)$, where the time units are hours. As in the previous example, we have added points $(0, 0)$ and $(168, n_i)$ at the beginning and at the end of each trajectory. The minimum and maximum observed numbers of bids for auctions in the sample are 8 and 51 respectively. Applying the algorithm described in Section 2.3, with results shown in Figure 6, indicates that the registered (non-standardized) intensity functions show a clear exponential-type pattern. We

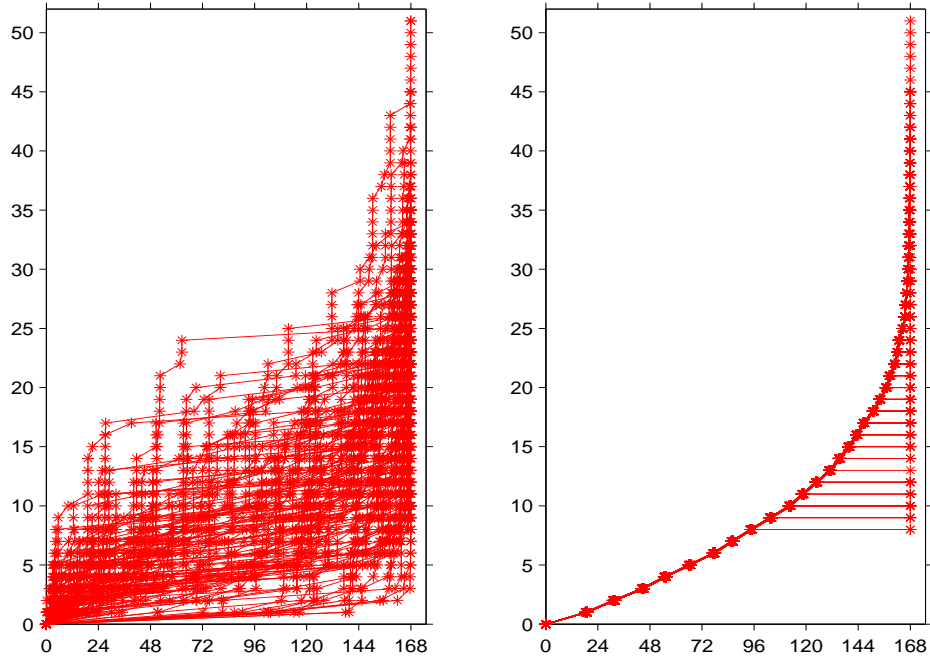


Figure 6: Left: Observed bidding trajectories Y_i for 156 auctions. Stars represent the observed data, solid lines are connecting the stars. Right: Registered bidding trajectories.

obtain an “almost common” intensity function irrespective of the number of bids. Indeed, the function is the same for all auctions except for the time period after the last bid, which is represented by a constant straight line at a height that depends on the total number of bids. This time period has been expanded (resp. contracted) during the registration process in those auctions with a low (resp. high) number of bids. Due to the low variability in the registered sample, the group mean intensity functions (Figure 7) look similar to the registered trajectories. Also in Figure 7, the overall mean intensity function after registration is compared to the sample mean of the observed curves. We can appreciate how “early bidding” and “bid sniping” emerge as phenomena that are due to time warping of the overall mean intensity function.

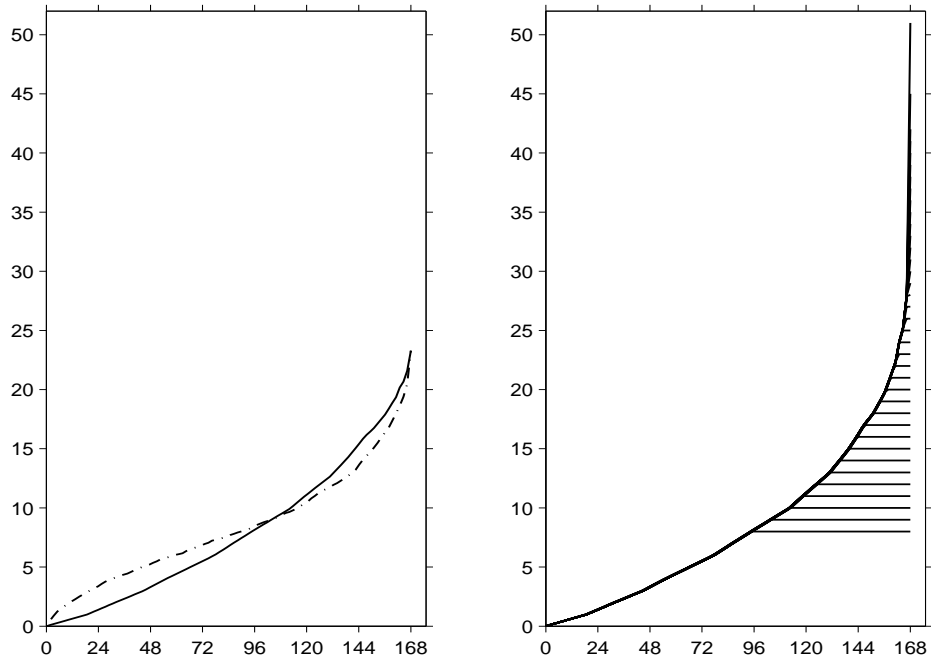


Figure 7: Left: Mean intensity function before (dashed-dotted line) and after registration (solid line). Right: Group mean intensity functions. The grouping is defined by the number of bids.

Aiming to differentiate between different bidding behaviors, we apply the warping-based clustering procedure described in Section 3.1. Here, again the number of clusters was found to be $k = 2$, with a *silhouette* coefficient of 0.65. In Figure 8 we present the warping function estimates, bidding trajectories and final price distributions of the two clusters. In fact, we want to investigate any possible relation between the bidding dynamics and the closing price of an auction. The clusters are defined by auctions with late (“L”) and regular-early (“R-E”) bidding activity. This is obvious if we look at the warping function estimates corresponding to each group. However, it is more difficult to tell the differences between the observed bidding trajectories of the two clusters. Some of them, although classified in different groups may be close together in terms of an L^2 distance on the space of observed trajectories. Then, the warping-based clustering provides a useful tool for understanding bidding activity. The first cluster, “L”, is composed by auctions with a very slow start, and contains most of the auctions with lowest final prices. Indeed the median final price of cluster “L” is slightly lower than that of “R-E”. However it also contains auctions with high closing prices (ranging between 240 and 260 \$), although these systematically correspond to auctions with unusually high opening bids (ranging between 50 and 179.99 \$). The second cluster, “R-E”, contains both auctions with bidding trajectories that are similar to the mean intensity function obtained after registration and auctions presenting very intense early bidding activity. The bidding trajectories of the two groups seem to present a similar final shape (a very important increase in the bidding activity during the last day of the auction) up to a vertical shift. That is, bidders behavior during the last day of an auction seems to be the same independently of the previous bidding activity until that moment. According to this, one could think that the first hours of an auction determine its outcome. However, this may not be completely true. In fact, in cluster “R-E” one can distinguish two very different starting behaviors, which do not correspond to different price distributions. Indeed, if one chooses to divide the data into 3 groups, cluster “R-E” is split into an “R” and an “E” cluster for which the closing price distributions are very similar. As a conclusion, we could say that it is a very low activity during the first 3/4 of an auction that yields to lower closing prices. In contrast, auctions with an early intense

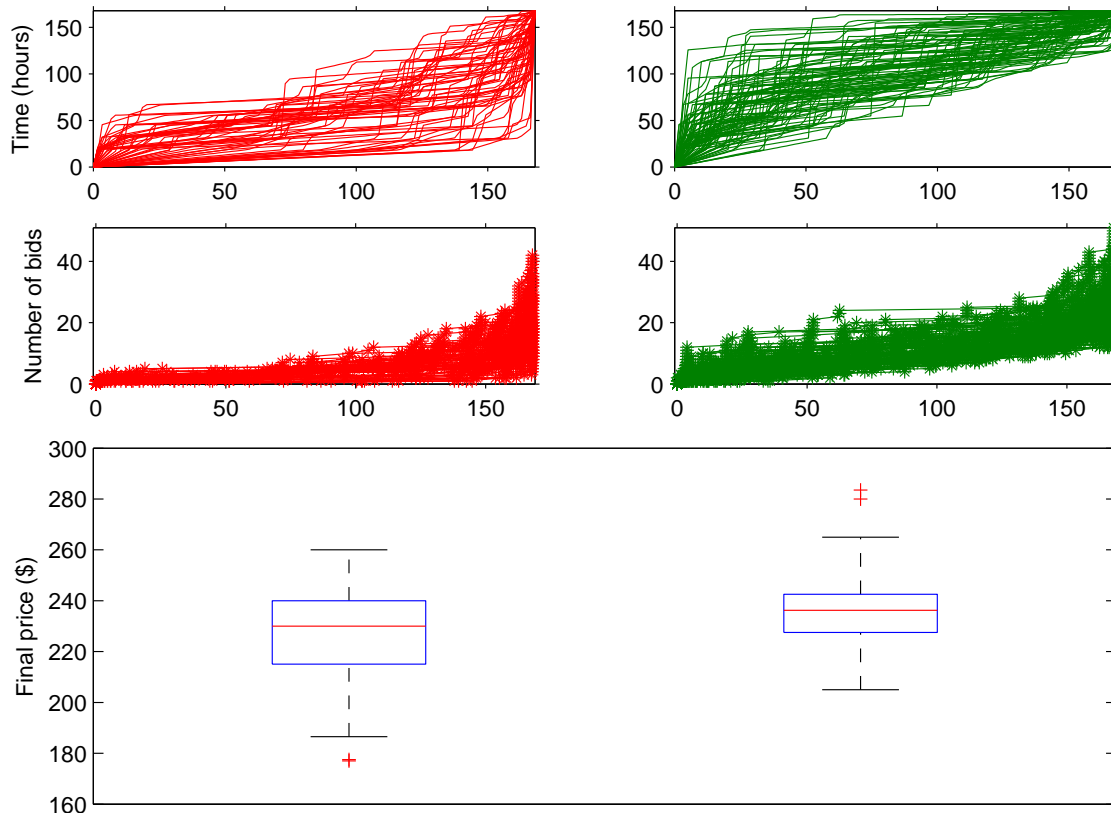


Figure 8: Warping function estimates (\hat{h}_i^{-1}), bidding trajectories and box plots of the final auction price for the two clusters “L” (left) and “R-E” (right).

bidding activity do not necessary lead to higher final prices than those with a regular starting.

4 Discussion

We have proposed an efficient registration algorithm for functional data that can be characterized by a random number of event times, which could correspond to original observations, or alternatively could be derived features from functional data such as the location of peaks, which are not consistently observed across the random trajectories that constitute the functional data sample. One of the advantages of

the proposed method is that it can cope with large sets of curves. Unlike previous DTW-based strategies for continuous time curve registration we focus on discrete time pairwise “local” alignments that subsequently are combined to obtain a whole sample “global” alignment.

The method relies on the choice of a metric on the observations space, which is used to find matching values over different curves. Throughout this article we consider the Euclidean distance for this purpose, although any other metric could be used. Indeed, this is a crucial point: different metrics will provide different alignments. Knowing which values should be aligned together is equivalent to having a notion of what similarity means in each particular application. For example, in the applications of Section 3, we focus on aligning some particular events, such as the birth of the first child, for the fertility data. For this purpose, the Euclidean distance proves to be quite suitable.

As for the clustering of a sample of curves, one may wonder why the distance-based method described in Section 3.1 is not directly applied to the observed curves instead of the warping estimates. Of course this could be done, but the results will be different, due to differences in the distance matrix used for clustering. Here again, different similarity notions can be suitable for different purposes. In this context, our proposal of clustering based on warping estimates can be seen as a way of defining a distance between individuals which focuses on similar temporal behavior.

Acknowledgments

This research was supported by NSF grants DMS-1104426 and DMS-1228369, and by Spanish grants “José Castillejo” JC2010-0057, MTM2010-17323 and ECO2011-25706 (Spanish Ministry of Science and Innovation).

References

J. Aach and G. M. Church. Aligning gene expression time series with time warping algorithms. *Bioinformatics*, 17:495–508, 2001.

- J. Bigot. Landmark-based registration of curves via the continuous wavelet transform. *Journal of Computational and Graphical Statistics*, 15:542–564, 2006.
- P. R. Bouzas, M. Valderrama, A. M. Aguilera, and Ruiz-Fuentes. Modeling the mean of a doubly stochastic Poisson process by functional data analysis. *Computational Statistics and Data Analysis*, 50:2655–2667, 2006.
- P. Clote and J. Straubhaar. Symmetric time warping, Boltzmann pair probabilities and functional genomics. *Journal of Mathematical Biology*, 53:135–161, 2006.
- T. Gasser and A. Kneip. Searching for structure in curve samples. *Journal of the American Statistical Association*, 90:1179–1188, 1995.
- Th. Gasser, W. Köhler, H.G. Müller, A. Kneip, R. Largo, L. Molinari, and A. Prader. Velocity and acceleration of height growth using kernel estimation. *Annals of Human Biology*, 11:397–411, 1984a.
- Th. Gasser, H.G. Müller, W. Köhler, L. Molinari, and A. Prader. Nonparametric regression analysis of growth curves. *Annals of Statistics*, 12:210–229, 1984b.
- D. Gervini and T. Gasser. Self-modeling warping functions. *Journal of the Royal Statistical Society, Ser. B*, 66:959–971, 2004.
- W. Jank and G. Shmueli. Functional data analysis in electronic commerce research. *Statistical Science*, 21:155–166, 2006.
- L. Kaufman and P. J. Rousseeuw. *Finding groups in data: An introduction to cluster analysis*. Wiley-Interscience, 1990.
- A. Kneip and T. Gasser. Statistical tools to analyze data representing a sample of curves. *The Annals of Statistics*, 16:82–112, 1992.
- A. Kneip and J.O. Ramsay. Combining registration and fitting for functional models. *Journal of the American Statistical Association*, 103(483):1115–1165, 2008.

- J.B. Kruskal and M. Liberman. The symmetric time-warping problem: From continuous to discrete. In J. B. Kruskal and D. Sankoff, editors, *Time warps, string edits, and macromolecules: The theory and practice of sequence comparison*, pages 125–161. Addison-Wesley, 1983.
- B. Liu and H. G. Müller. Functional data analysis for sparse auction data. In W. Jank and G. Shmueli, editors, *Statistical Methods in E-commerce research*, pages 269–290. Wiley, New York, 2008.
- X. Liu and H.G. Müller. Functional convex averaging and synchronization for time-warped random curves. *Journal of the American Statistical Association*, 99(467): 687–699, 2004.
- H. G. Müller, J. M. Chiou, J. R. Carey, and J. L. Wang. Fertility and lifespan: Late children enhance female longevity. *The Journals of Gerontology: Biological Sciences*, 57:202–206, 2002.
- S. B. Needleman and C. D. Wunsch. A general method applicable to the search for similarities in the amino acid sequences of two proteins. *Journal of Molecular Biology*, 48:443–453, 1970.
- T. Rong and H. G. Müller. Pairwise curve synchronization for functional data. *Biometrika*, 95(4):875–889, 2008.
- B. B. Rønn. Nonparametric maximum likelihood estimation for shifted curves. *Journal of the Royal Statistical Society, Ser. B*, 63:243–259, 2001.
- G. Shmueli and W. Jank. Visualizing online auctions. *Journal of Computational and Graphical Statistics*, 14:299–319, 2005.
- G. Shmueli, R. P. Russo, and W. Jank. The BARISTA: a model for bid arrivals in online auctions. *The Annals of Applied Statistics*, 1:412–441, 2007.
- B.W. Silverman. Incorporating parametric effects into functional principal components analysis. *Journal of the Royal Statistical Society, Ser. B*, 57:673–689, 1995.

- D. Telesca and L.Y.T. Inoue. Bayesian hierarchical curve registration. *Journal of the American Statistical Association*, 103(481):328–339, 2008.
- K. Wang and T. Gasser. Alignment of curves by dynamic time warping. *The Annals of Statistics*, 25:1251–1276, 1997.
- K. Wang and T. Gasser. Synchronizing sample curves nonparametrically. *Annals of Statistics*, 27:439–460, 1999.
- H. Wu, S. Müller and Z. Zhang. Functional data analysis for point processes with rare events. *Statistica Sinica*, in press, 2012.
- Z. Zhang and H.-G. Müller. Functional density synchronization. *Computational Statistics and Data Analysis*, 55:2234–2249, 2011.